



Published in final edited form as:

*J Immunol.* 2016 September 1; 197(5): 1864–1876. doi:10.4049/jimmunol.1600410.

## Zinc Induces Dendritic Cell Tolerogenic Phenotype and Skews Regulatory T cell – Th17 Balance

Mariam Mathew George<sup>1,¥</sup>, Kavitha Subramanian Vignesh<sup>2,¥</sup>, Julio A. Landero Figueroa<sup>3</sup>, Joseph A. Caruso<sup>3</sup>, and George S. Deepe Jr<sup>2,4,\*</sup>

<sup>1</sup>Division of Immunobiology, Cincinnati Children's Hospital Medical Center, Cincinnati, OH 45229 USA

<sup>2</sup>Division of Infectious Diseases, College of Medicine, University of Cincinnati, Cincinnati, OH 45267 USA

<sup>3</sup>University of Cincinnati/Agilent Technologies Metallomics Center of the Americas, Department of Chemistry, University of Cincinnati, Cincinnati, OH 45221 USA

<sup>4</sup>Veterans Affairs Hospital, Cincinnati, OH 45220 USA

### Abstract

Zn is an essential metal for development and maintenance of both the innate and adaptive compartments of the immune system. Zn homeostasis impacts maturation of dendritic cells (DCs) that are important in shaping T cell responses. The mechanism by which Zn regulates the tolerogenic phenotype of DCs remains largely unknown. In this study, we investigated the effect of Zn on DC phenotype and the generation of forkhead box P3 (FoxP3<sup>+</sup>) regulatory T cells (Tregs) using a model of *Histoplasma capsulatum* fungal infection. Exposure of bone marrow derived DCs to Zn *in vitro* induced a tolerogenic phenotype by diminishing surface major histocompatibility complex (MHC)II and promoting the tolerogenic markers, programmed death-ligand (PD-L)1, PD-L2 and the tryptophan degrading enzyme, indoleamine 2,3 dioxygenase (IDO). Zn triggered tryptophan degradation by IDO and kynurenine production by DCs and strongly suppressed the proinflammatory response to stimulation by toll like receptor (TLR) ligands. *In vivo*, Zn supplementation and subsequent *H. capsulatum* infection suppressed MHCII on DCs, enhanced PD-L1 and PD-L2 expression on MHCII<sup>lo</sup> DCs and skewed the Treg - Th17 balance in favour of FoxP3<sup>+</sup> Tregs while decreasing Th17 cells. Thus, Zn shapes the tolerogenic potential of DCs *in vitro* and *in vivo* and promotes Tregs during fungal infection.

\*Correspondence: George S. Deepe, Jr. MD, george.deepe@uc.edu, Phone 5135584706, Fax-5135582089.

¥These authors contributed equally to this work.

The authors declare no conflicts of interest.

#### Author Contributions

M.M.G and K.S.V provided equal contributions to the work and wrote the manuscript, M.M.G performed *in vitro* and *in vivo* experiments and analyzed data, K. S. V designed and supervised the study, performed *in vivo* experiments and interpreted data, J.A.L.F. performed tryptophan degradation analysis by HPLC. K.S.V and G.S.D. supervised the work.

## Introduction

Dendritic cells (DCs) play an important role in bridging innate and adaptive immune responses. DCs constitute a heterogeneous population that exert diverse functions in immune regulation and are distinguished by various surface and intracellular markers (1). They recognize and respond to environmental cues such as pathogens, and phagocytose and present antigens to drive effector T cell responses (1). More recently, DCs have been demonstrated to control inflammation by promoting tolerance. This subset, referred to as tolerogenic DCs, mediates inflammation control and shapes the regulatory phenotype of T cells. (2).

Zn plays a crucial role in homeostasis and optimal function of the innate and adaptive compartments of the immune system (3). The metal acts as an intracellular signaling molecule and regulates the functions of several myeloid and lymphoid populations (4). Both Zn deficiency and supplementation have profound effects on the development and function of T cells, B cells, natural killer (NK) cells, monocytes and macrophages. For example, Zn deficiency inhibits NK cell lytic activity, T helper 1 (Th1) cytokine production and B cell responses (4, 5). Conversely, Zn supplementation can regulate immune responses during infection by limiting excessive production of proinflammatory cytokines and uncontrolled inflammation (6). Regulation of Zn homeostasis also affects DC maturation (7). Upon activation in response to infectious agents or other proinflammatory stimuli, DCs mature and elevate MHCII to subsequently drive T cell proliferation and differentiation (8). In response to TLR4 stimulation by lipopolysaccharide (LPS), DCs decrease their intracellular free Zn pool to elevate surface MHCII expression. Conversely, exogenous Zn supplementation decreases MHCII on the surface of DCs possibly through endocytosis and decreased vesicular transport of the protein (9).

Proinflammatory or regulatory response of DCs is accompanied by the expression of activation or tolerogenic markers respectively (8). In order to control excessive inflammation, tolerance mechanisms are important especially at sites of infection. DCs inhibit T cell effector responses through mechanisms that include production of anti-inflammatory factors such as transforming growth factor  $\beta$  (TGF $\beta$ ) and interleukin (IL)-10. These cytokines suppress effector T cell function and induce Tregs that mitigate inflammation, maintain tolerance to self-antigens and control autoimmunity (10). The inhibition of effector T cell responses is mediated by tolerogenic DCs that express the co-inhibitory molecules, PD-L1 and PD-L2 which engage the PD-1 receptor on T cells to induce a regulatory phenotype (10, 11). The tryptophan degrading enzyme, IDO produced by tolerogenic DCs suppresses inflammation via effector T cell apoptosis and promotes Treg development (10, 12). Thus, an adequate balance of effector T cells and Treg function is necessary to maintain tissue homeostasis under pathological conditions. However, the factors that induce inhibitory markers on DCs to mediate a tolerogenic phenotype remain obscure.

The fungal pathogen, *Histoplasma capsulatum* causes pulmonary infection in healthy individuals and disseminated infection in immunocompromised patients (13). DCs recognize *H. capsulatum* via the fibronectin receptor, very late antigen-5 (VLA-5) or alpha 5 beta 1

integrin and present antigens to trigger a Th1 response (14). Unlike resting macrophages, DCs phagocytose yeasts, inhibit fungal growth and activate Th1 immunity to mediate clearance of the pathogen. In this context, the role of metal ions in mitigating excessive inflammation and uncontrolled production of proinflammatory mediators by DCs during infection has not been determined.

In this study, we investigated the role of Zn in shaping the DC phenotype and its impact on T cell differentiation using *H. capsulatum* as a prototypic fungal pathogen. We reveal that Zn programs the tolerogenic potential of DCs *in vitro* and *in vivo* by suppressing MHCII and promoting the expression of tolerogenic markers. *In vivo*, upon pulmonary fungal challenge, Zn supplementation skewed the Treg-Th17 balance towards Tregs while concomitantly decreasing Th17 cells. Lastly, we uncover that Zn severely impairs the ability of DCs to mount a proinflammatory response to fungal infection and stimulation by TLR ligands. Thus, Zn shapes the tolerogenic phenotype of DCs and promotes the generation of Tregs.

## Materials and Methods

### Mice

C57BL/6 and FoxP3<sup>GFP</sup> mice were obtained from Jackson laboratory. *Irf8*<sup>-/-</sup> and *Ifnar1*<sup>-/-</sup> mice were kindly provided by Dr. Harinder Singh and Dr. Edith Janssen at Cincinnati Children's Hospital Medical Center (CCHMC), respectively. Animals were maintained by the Department of Laboratory Animal Medicine, University of Cincinnati, accredited by the American Association for Accreditation of Laboratory Animal Care (Frederick, MD). All animal experiments were in accordance with Animal Welfare Act guidelines of National Institutes of Health.

### *In vitro* DC preparation and *H. capsulatum* infection

Bone marrow from femurs and tibias of ~8–12 week old mice were cultured in RPMI (BioWhittaker, MD) with 10% fetal bovine serum (HyClone Laboratories, Utah), 0.005% 2-mercaptoethanol, 10 mg/L gentamicin (MP Biomedicals, LLC) and 10 ng/ml GM-CSF (Peprotech) for 6 days at 37°C and 5% CO<sub>2</sub>. DCs were isolated from floating cells using CD11c magnetic bead isolation (Miltenyi Biotec) and treated with 100 μM ZnSO<sub>4</sub> (Sigma-Aldrich) and infected with *H. capsulatum* (217B) at a multiplicity of infection (MOI) of 0.5 yeasts per DC for 24 h at 37°C. Cells were harvested after 24 h for gene expression analysis or flow cytometry.

### Cell viability

DCs were isolated from floating cells using CD11c magnetic bead isolation (Miltenyi Biotec) and treated with 100 μM ZnSO<sub>4</sub> (Sigma-Aldrich) and infected with an MOI of 0.5 yeasts for 24 h at 37°C. Cells were washed with 0.5% bovine serum albumin in PBS (pH 7.4) and stained with 5 μl 7AAD stain/10<sup>6</sup> cells for 5 mins at 4°C and analyzed by flow cytometry (Accuri C6). Data were analyzed using FCS Express 4, De Novo Software (CA).

## Gene expression

Genomic DNA was removed using gDNA eliminator mini spin columns and RNA was extracted using RNeasy micro kit (Qiagen). cDNA was prepared using Reverse Transcription Systems kit (Promega, WI). qRT-PCR was performed in ABI Prism 7500, using Taqman assay with primer and probe sets from Applied Biosystems, CA. Hypoxanthine guanine phosphoribosyl transferase (*Hprt*) was used as internal standard and target gene expression was normalized to control untreated and uninfected bone marrow derived DCs.

## Flow cytometry

CD11c fluorescein isothiocyanate (FITC)-, CD11c allophycocyanin- (APC), Ia-Ie phycoerythrin (PE), IA-b APC, CD103 PE, TLR4 PE, F4/80 APC, CD11b PE, CD8 PE and CD4 APC were purchased from BD Biosciences and Biotin-conjugated PDL1<sup>+</sup>, PD-L2<sup>+</sup> and APC-conjugated Streptavidin were from BioLegend. For surface staining, cells were washed with 0.5% bovine serum albumin in PBS (pH 7.4) and stained at 4°C for 15 min. in the presence of CD16/32 blocking antibodies. To characterize Th1, Th2 and Th17 cells, lung leukocytes were stimulated with 50 ng/ml of phorbol 12-myristate 13-acetate (PMA), 500 ng/ml ionomycin and 10 µg/ml brefeldin A (BFA) for 6 h *in vitro* and stained for surface markers as above followed by fixation and permeabilization with Cytofix/Cytoperm (BD Biosciences) for 20 mins at 4°C, washed in permeabilization buffer (BD Biosciences), and stained for 1 hour with IFN $\gamma$ , IL-4 and IL-17A PE antibodies (BD Biosciences). Cells were characterized using flow cytometry (Accuri C6). Data were analyzed in FCS Express 4 Software, De Novo (CA).

## DC sorting

DCs were purified using CD11c magnetic beads (Miltenyi biotec) and identified by gating on the CD11c<sup>+</sup> MHCII<sup>+</sup> population. DCs were sorted into MHCII high (MHCII<sup>hi</sup>) and MHCII low (MHCII<sup>lo</sup>) on a MoFlo sorter (Dako) at Cincinnati Children's Hospital Medical Center. The sorted MHCII<sup>hi</sup> and MHCII<sup>lo</sup> cells were plated with 100 µM ZnSO<sub>4</sub> and infected with an MOI of 0.5 *H. capsulatum* yeasts per DC for 24 h at 37°C. Cells were harvested for gene expression and tryptophan degradation assay.

## Tryptophan degradation assay

2×10<sup>6</sup> CD11c<sup>+</sup> DCs were treated with 100 µM ZnSO<sub>4</sub> and infected for 24 h following which the cells were collected and incubated in 500 µl of 100 µM L-tryptophan (Sigma-Aldrich) in sterile DDI H<sub>2</sub>O (pH 7.5) or 100 µM/ml 1-Methyl L-Tryptophan (1-MT, Sigma-Aldrich) prepared in 2% acetic acid (pH 7.5) at 37°C overnight on a rocker. Next day, the mixture was incubated at 55°C for 30 min. Samples were spun down at 13,000 × *g* to remove cell debris and immediately stored at -80°C prior to high performance liquid chromatography (HPLC) analysis.

HPLC analysis of tryptophan and kynurenine was performed on an 1100 Agilent liquid chromatographer equipped with a vacuum membrane degasser, a binary pump, a thermostated autosampler an oven column compartment, a UV-Vis Diode array detector and a diode array fluorescence detector. All modules were connected by 0.17 mm ID PEEK

tubing and controlled with ChemStation software. A Zorbax Extend C-18 column,  $4.6 \times 250$  mm,  $5 \mu\text{m}$  particle size was used with a C-18 pre-column cartridge. The method was adapted from Winder et al (15). In brief, proteins were precipitated from the samples in amber vials by adding trichloroacetic acid a final concentration of 5 mM. After centrifugation at  $13,000 \times g$  for 10 min. the supernatant was diluted 1:1 with mobile phase, filtered through  $0.45 \mu\text{m}$  spin filter at  $10,000 \times g$  for 5 min. and injected into the HPLC system. The mobile phase consisted of potassium phosphate 15 mM at pH 6.4. Kynurenine was detected by UV-Vis at 360 nm, while the tryptophan was detected by a fluorescence detector with the excitation wavelength of 285 nm and the emission wavelength of 365 nm. Calibration standards were used in the range of  $0.5 \mu\text{M}$  to  $100 \mu\text{M}$  to quantify the two species.

### TLR stimulation

CD11c<sup>+</sup> DCs were treated with  $100 \mu\text{M}$  ZnSO<sub>4</sub> and infected with 0.5 *H. capsulatum* per DC for 24 h. Cells were then treated with 100 ng/ml lipopolysaccharide (LPS) (Sigma-Aldrich) for 4 h and 6 h or  $10 \mu\text{g/ml}$  polyinosinic:polycytidylic acid (Poly I:C) (InvivoGen) for 4 h or  $10 \mu\text{g/ml}$  peptidoglycan from *Staphylococcus aureus* (PGN-SA) (InvivoGen) for 4 h. After TLR stimulation, culture supernatants were centrifuged at 1600 rpm for 5 min. Cell free supernatant was collected for cytokine studies and cells were processed for gene expression analysis. Supernatants were analyzed for cytokines by Milliplex multiplex assay using Luminex (Millipore).

### In vivo Zn supplementation and infection

Eight to twelve week-old FoxP3<sup>GFP</sup> mice were injected intraperitoneally (*i.p.*) with double distilled water (DDI H<sub>2</sub>O) or  $100 \mu\text{g}$  ZnSO<sub>4</sub> (Sigma-Aldrich) dissolved in DDI H<sub>2</sub>O daily for 7 days and then infected with a sub lethal dose of  $2 \times 10^6$  *H. capsulatum* (217B) yeasts intranasally (*i.n.*). ZnSO<sub>4</sub> and DDI H<sub>2</sub>O treatment continued daily during the period of infection for 7 days, 14 days or 21 days. At these time points, mice were sacrificed and the lungs, spleens and mediastinal lymph nodes were harvested for leukocyte isolation and assessment of fungal burden. Lung homogenates were also collected for measuring cytokines by Milliplex multiplex assay using Luminex (Millipore) or by ELISA. For analysis of lung pathology, mouse lungs were harvested 14 days *p.i.*, fixed, embedded in paraffin blocks, sectioned and stained with H&E for analysis.

### Isolation of leukocytes

Mediastinal lymph nodes and spleens were homogenized using frosted glass slides in HBSS. Lungs were homogenized in 5 ml HBSS using a gentleMACS Dissociator (Miltenyi Biotec), collagenase treated ( $0.01 \text{ g/lung}$ ) for 30 mins on a rocker, filtered through  $70 \mu\text{m}$  nylon mesh (Fisher Scientific) and leukocytes were isolated by density gradient separation using Lympholyte M (Cedarlane Laboratories). Cells were stained for analysis by flow cytometry or lysed for RNA isolation and gene expression analysis.

### Organ cultures for fungal burden

Mice were sacrificed on days 7, 14 or 21 post infection (*p.i.*) and lungs and spleens were homogenized as above. Organ homogenates were plated on Mycosel agar plates (Becton

Dickenson Company, Sparks, MD) supplemented with agarose (8 g/L), dextrose (10 g/L), cysteine (100 µg/L) and defibrinated sheep blood (50 ml/L). Plates were incubated at 37°C for 7 days and fungal colonies were enumerated.

### Treg differentiation

CD4<sup>+</sup>CD62L<sup>+</sup> naïve T cells were isolated from spleens and lymph nodes of 8–15 weeks old FoxP3<sup>GFP</sup> mice using magnetic beads (Miltenyi Biotec) and co-cultured with the DCs with or without IL-2 and TGFβ and ZnSO<sub>4</sub>. After 5 days, cells were harvested and stained for CD4 using the above mentioned staining protocol and analyzed by FACS for FoxP3 GFP expression.

### Statistical analysis

*p* values for multiple comparisons were calculated using one-way ANOVA or three-way ANOVA and adjusted with Holm Sidak or Bonferroni's correction. For comparison of two groups, non-paired Student's *t* test was used; \* *p* < 0.05; \*\* *p* < 0.01; \*\*\* *p* < 0.001; and NS, not significant.

## Results

### Zn suppresses surface MHCII expression on DCs

Stimulation of pathogen recognition receptors on DCs induces an increase in MHCII and promotes DC maturation. Stimulation of DCs with the TLR4 ligand, LPS, decreases the intracellular Zn pool leading to elevated MHCII surface expression (9). To understand how Zn regulated the maturation status of DCs, we sought to study the effect of Zn on DCs in the resting state and upon infection with *H. capsulatum*. CD11c<sup>+</sup> bone marrow derived DCs were exposed to Zn and left uninfected or simultaneously infected with yeasts for 24 h to determine changes in surface MHCII. Zn exposure decreased the proportion of MHCII<sup>hi</sup> DCs and increased MHCII<sup>lo</sup> DCs in the resting state. This observation is consistent with the report that Zn inhibits MHCII expression on DCs (9). Upon infection, untreated DCs exhibited an increase in MHCII<sup>hi</sup> and a corresponding decrease in MHCII<sup>lo</sup> population. Zn treatment however, abrogated the shift in MHCII expression leading to a larger proportion of MHCII<sup>lo</sup> DCs and a decrease in the mean fluorescence intensity (MFI) of MHCII upon infection (Figs. 1A and 1B). We queried whether Zn supplementation affected DC viability. *H. capsulatum* infected DCs treated with Zn exhibited similar viability after 24 h compared to their respective controls (Supplemental Fig. 1A).

### Zn induces generation of a tolerogenic DC phenotype

We hypothesized that a decrease in MHCII surface expression alters the maturation state of DCs that in turn promotes their tolerogenic potential. Thus, we investigated whether Zn modulated the tolerogenic potential of DCs by assessing PD-L1 and PD-L2 on MHCII<sup>hi</sup> and MHCII<sup>lo</sup> DCs. Zn did not alter the percentage of PD-L1<sup>+</sup> DCs in these compartments and the MFI of PD-L1 in MHCII<sup>lo</sup> DCs was only marginally increased by Zn upon infection (Fig. 2A, 2D and 3A). Next, we investigated whether Zn modulated PD-L2 expression. There was a significant elevation in the percentage of PD-L2<sup>+</sup> MHCII<sup>lo</sup> in uninfected (*p* < 0.001) and infected (*p* < 0.01) DCs exposed to Zn, and a corresponding reduction in the

proportion of PD-L2<sup>+</sup> MHCII<sup>hi</sup> DCs (Fig. 2B and 2D). Zn significantly augmented the MFI of PD-L2 in MHCII<sup>lo</sup> uninfected ( $p < 0.001$ ) and infected DCs ( $p < 0.01$ ) and diminished the expression of this marker in MHCII<sup>hi</sup> DCs (Fig. 3B).

CD103<sup>+</sup> DCs in the lung, pancreas and liver induce T cell migration with tropism for these specific sites (16). This subset of DCs promotes FoxP3<sup>+</sup> Tregs in a retinoic acid and TGF $\beta$  dependent manner in the gut (17). We therefore sought to probe the expression of CD103 on DCs in response to Zn. Although the proportions of CD103<sup>+</sup> MHCII<sup>hi</sup> and CD103<sup>+</sup> MHCII<sup>lo</sup> DCs were not changed (Fig. 2C and 2D), Zn induced a significant increase ( $p < 0.01$ ) in CD103 MFI specifically in uninfected MHCII<sup>lo</sup> DCs (Fig. 3C). We asked whether Zn modulated the expression of Notch ligand genes, *Jag1*, *Jag2* and *delta like ligand 4 (Dll4)* in DCs as these molecules mediate the induction of Tregs or Th2 cells through the Notch signaling pathway under specific conditions (18). The expression of *Jag1*, *Jag2* and *Dll4* on DCs was not modified by Zn (Supplementary Fig. 1B). These data indicate that Zn suppresses MHCII expression and induces tolerogenic markers on DCs.

### Zn triggers tryptophan degradation by DCs

IDO is the first and rate-limiting enzyme driving tryptophan catabolism through the kynurenine pathway. IDO produced by tolerogenic DCs depletes tryptophan to limit microbial growth and T cell survival (10). Kynurenine metabolites produced as a result of tryptophan degradation by IDO induce Tregs and TGF $\beta$  expression in DCs (19). To probe whether Zn regulated this tolerogenic marker in DCs, we analyzed *Ido1* expression and function in DCs exposed to the metal. *Ido1* mRNA was elevated as early as 6 h post Zn treatment. At 24 h, Zn significantly induced a 3.5 fold elevation in *Ido1* expression in uninfected ( $p < 0.001$ ) and infected DCs ( $p < 0.05$ ) (Fig. 4A). We asked if *Ido1* expression depended on the Zn concentration. The expression of *Ido1* was unaltered by 0.1  $\mu$ M and 10  $\mu$ M of ZnSO<sub>4</sub>, but increased upon treatment with 100  $\mu$ M ZnSO<sub>4</sub> (Supplementary Fig. 2A). To determine if Zn specifically induced IDO in MHCII<sup>lo</sup> DCs, we sorted MHCII<sup>hi</sup> and MHCII<sup>lo</sup> DCs and stimulated them with Zn for 24 h. The induction of *Ido1* transcription by Zn in MHCII<sup>hi</sup> and MHCII<sup>lo</sup> DCs was comparable (Supplementary Fig. 2B). To determine if the IDO response was specific to Zn, we exposed DCs to iron sulfate (FeSO<sub>4</sub>). This divalent cation failed to trigger *Ido1* expression in DCs indicating that this tolerogenic marker was specifically induced by Zn (Supplementary Fig. 2C).

To investigate the functional importance of IDO induction we incubated Zn-treated DCs with L-tryptophan and assessed amino acid degradation and concomitant kynurenine production. Consistent with an elevation in *Ido1* expression, Zn-treated DCs augmented degradation of tryptophan into the downstream metabolite, kynurenine (Fig. 4B, 4D). We exposed DCs to 1-methyl L-tryptophan (1-MT), a competitive inhibitor of IDO activity. 1-MT completely blocked tryptophan degradation and conversion to kynurenine by Zn-treated DCs (Fig. 4B). Moreover, MHCII<sup>lo</sup> DCs degraded tryptophan comparably to unsorted DCs (Fig. 4C, 4D). These data substantiate the role of Zn in promoting IDO function in DCs and reveal the emergence of a tolerogenic phenotype.

We investigated the molecular signals that regulate IDO induction by Zn. *Ido1* expression is driven by the interferon regulatory factor 8 (IRF8) transcription factor in DCs (20). To

determine if IRF8 was involved, we treated wild type (WT) and *Irf8*<sup>-/-</sup> DCs with Zn. IRF8 deficiency completely abrogated the increase in *Ido1* transcription by Zn compared to WT DCs (Fig. 5A). Type I interferons like IFN $\alpha$  and IFN $\beta$  also induce IDO in DCs and macrophages (21, 22). To examine their role, we treated DCs from IFN receptor 1 knockout (*Ifnar1*<sup>-/-</sup>) mice with Zn and infected them for 24 h. *Ido1* expression was attenuated in uninfected and infected *Ifnar1*<sup>-/-</sup> DCs at baseline as well as in response to Zn (Fig. 5B). To test if Zn induced *Ifnb*, WT DCs were treated with Zn and infected for 24 h. *Ifnb* expression was upregulated only upon infection and not as a result of Zn treatment (Fig. 5C). These data indicate that Zn regulates IDO via IRF8 and IFNAR signaling pathways in DCs.

### Zn suppresses proinflammatory phenotype of DCs

Our data suggested that the Zn-induced tolerogenic phenotype in DCs would result in a blunted proinflammatory response. Thus, we asked whether this metal affected the ability of DCs to respond to proinflammatory stimuli. Zn treated and infected DCs were stimulated with LPS, peptidoglycan derived from *Staphylococcus aureus* (PGN-SA) or polyinosinic:polycytidylic acid (Poly I:C) to target TLR 4, 2 or 3 respectively. Zn impaired the TLR4 response to LPS in uninfected DCs leading to diminished expression of *Il-1b*, *Il6*, nitric oxide synthase 2 (*Nos2*), *Il12a* and *Il12b*. *Tnfa* expression was also marginally reduced upon Zn treatment. *H. capsulatum* infected DCs potently induced transcription of proinflammatory cytokine genes, but Zn exposure resulted in a markedly poor proinflammatory response to infection with decreased expression of *Il1b*, *Il6*, *Tnfa*, *Nos2*, *Il12a* and *Il12b*. The expression of *Il10* remained unaltered (Fig. 6A). In contrast, arginase 1 (*Arg1*) expression was enhanced in Zn-treated uninfected and infected DCs, an effect that was dampened by TLR4 stimulation (Fig. 6A). Exposure to Zn diminished IL-6 production (Fig. 6B). The reduction in LPS mediated proinflammatory response by Zn was not a result of altered TLR4 surface expression (Fig. 6C).

TLR2 and TLR4 receptors signal in a MyD88 and TIR-domain-containing adapter-inducing interferon- $\beta$  (TRIF) dependent manner, while TLR3 signals via a MyD88 independent pathway (23). To understand whether Zn inhibited MyD88 or TRIF signaling, or both, we queried whether Zn suppressed the proinflammatory response of DCs to TLR2 and TLR3 ligands. *Il1b*, *Il6*, *Tnfa*, *Nos2*, *Il12a* and *Il10* genes were robustly induced by TLR2 and TLR3 ligands especially in infected DCs, but severely impaired by Zn treatment (Fig. 7A and 7C). Stimulation with these ligands partially suppressed the Zn-induced *Arg1* response (Fig. 7A and 7C). We detected a decrement in IL-1 $\beta$  and IL-6 proteins released in supernatant by Zn treated DCs upon TLR2 and TLR3 stimulation (Fig. 7B and 7D). These data indicate that Zn not only inhibits responsiveness to bacterial and viral antigens, but also impairs proinflammatory responses of DCs to fungal challenge.

### Zn impairs DC maturation and skews Treg-Th17 balance *in vivo*

We asked whether Zn induced a tolerogenic phenotype in DCs *in vivo*. Zn supplementation studies in mice have used doses ranging from 100–300 mg/kg (24, 25). For our *in vivo* studies, through preliminary analysis we determined that 100  $\mu$ g ZnSO<sub>4</sub>/mouse/day was optimal for assessing changes in DCs and T cells without impacting animal body weight or survival. FoxP3<sup>GFP</sup> mice were treated with 100  $\mu$ g ZnSO<sub>4</sub> or DDI H<sub>2</sub>O followed by infection



with *H. capsulatum* yeasts. We analyzed leukocytes from lung and mediastinal lymph nodes for macrophages, DCs, CD4<sup>+</sup> and CD8<sup>+</sup> cells on days 7, 14 and 21 post infection (*p.i.*) (Schematic, Fig. 8A). *In vivo*, Zn decreased the proportion of MHCII<sup>hi</sup> DCs while correspondingly elevating the percentage of MHCII<sup>lo</sup> DCs in lungs on day 14 *p.i.* (Fig. 8B). Consistent with our *in vitro* finding, Zn supplementation *in vivo* significantly decreased MHCII MFI on CD11c<sup>+</sup> DCs on day 7 and day 14 ( $p < 0.01$ ) post *H. capsulatum* infection (Fig. 8C). The percentage of macrophages, DCs, CD4 and CD8 cells in lungs were unaltered by Zn treatment (Fig. 8D). As Zn induced PD-L1 and PD-L2 in MHCII<sup>lo</sup> DCs *in vitro*, we assessed changes in these markers *in vivo*. The total percent of PD-L1<sup>+</sup> and PD-L2<sup>+</sup> DCs in the lungs were similar between DDI H<sub>2</sub>O and ZnSO<sub>4</sub> treated mice (Supplementary Fig. 3A). In agreement with our *in vitro* finding, Zn supplementation elevated the proportion of PD-L1 and PD-L2 expressing MHCII<sup>lo</sup> DCs, while decreasing PD-L1 and PD-L2 expressing MHCII<sup>hi</sup> DCs *in vivo* at day 14 *p.i.* (Supplementary Fig. 3B)

We asked whether Zn supplementation affected growth of *H. capsulatum* *in vivo* and found no changes in fungal burden in the lungs and spleens of mice on day 7 or 14 *p.i.* (Supplementary Fig. 3C). Pathological analysis of infected lungs revealed subtle differences in the ratio of lymphocytes to macrophages in the lesions, but no marked differences in the histologic features of the inflammatory response were observed upon Zn supplementation (data not shown).

We found that Zn supplementation significantly enhanced the proportion of CD4<sup>+</sup>FoxP3<sup>+</sup> Tregs on day 14 *p.i.* in the lungs ( $p < 0.05$ ) (Fig. 9A). Thus, we queried if Zn exposure skewed the Treg-Th17 balance during fungal infection. The increase in FoxP3<sup>+</sup> Tregs was accompanied by a significant decrease in IL-17 producing CD4<sup>+</sup> T cells ( $p < 0.01$ ) in *H. capsulatum* infected mouse lungs (Fig. 9B). Zn supplementation did not alter IFN $\gamma$  producing Th1 or IL-4 producing Th2 cells in lungs (Fig. 9C). Moreover, the increase in Tregs was specific to the site of infection as the proportion of Tregs was comparable in mediastinal lymph nodes (MLNs) of DDI H<sub>2</sub>O and Zn treated mice on day 14 *p.i.* (Supplementary Fig. 3D). To examine the possibility that Zn supplementation directly impacted T cell differentiation to increase Tregs, we isolated naïve T cells from FoxP3<sup>GFP</sup> mice and differentiated them into Tregs *in vitro* in the presence or absence of Zn. We found that Zn did not enhance the FoxP3<sup>GFP</sup> signal in naïve T cells or in cells differentiated in the presence of the Treg inducing cytokines, IL-2 and TGF $\beta$ , suggesting that the metal did not directly influence Treg differentiation *in vitro* (Supplementary Fig. 3E). These data indicate that Zn supplementation suppressed DC maturation and skewed the Treg-Th17 balance *in vivo* upon pulmonary fungal infection.

As exposure to Zn heightened IDO expression and function *in vitro*, we hypothesized that exogenous Zn supplementation would induce *Ido1* *in vivo*. There was a significant 4-fold upregulation ( $p < 0.05$ ) in *Ido1* expression in lung leukocytes of Zn treated mice compared to DDI H<sub>2</sub>O treated mice infected with *H. capsulatum* (Fig. 9D). The *Raldh1* gene encodes retinal dehydrogenase enzyme that converts vitamin A to its biologically active metabolite all-*trans* retinoic acid (RA). RA production by DCs and alveolar macrophages along with TGF $\beta$  promotes the differentiation of naïve T cells into Tregs (17, 26). We observed an increase in *Raldh1* expression in the lung leukocytes of Zn treated mice infected with *H.*

*capsulatum* (Fig. 9D). Moreover, in line with the skewed Treg-Th17 balance, leukocytes from Zn treated mice exhibited significantly diminished ( $p < 0.01$ ) *III7a* expression and *III7f* was comparable between DDI H<sub>2</sub>O and Zn treated mice (Fig. 9E). *Ifng*, *Ifnb*, *Il4*, *Il6*, *Il10* and *Tgfb* transcripts were not affected, but *Il2* was significantly reduced ( $p < 0.001$ ) by Zn supplementation (Fig. 9E and 9F). The production of IL-6, IL-12 (p40), IL-10 and TGF $\beta$  proteins remained unaltered in whole lung homogenates of Zn treated mice compared to DDI H<sub>2</sub>O treated mice (Supplementary Fig. 3F).

*H. capsulatum* infection subsides after 14 days and yeasts are cleared within 21 days. We therefore extended our analysis to this time point. MHCII expression on DCs, proportions of Tregs and fungal burden in the lungs were similar between DDI H<sub>2</sub>O and ZnSO<sub>4</sub> treated mice 21 days *p.i* (Supplementary Fig. 4A–E). Thus, Zn supplementation modulated the inflammatory response during the onset and peak of infection (days 7 and 14 respectively). This effect subsided with clearance of the pathogen. Collectively, these findings reveal that Zn programs the tolerogenic phenotype of DCs while suppressing their inflammatory capacity and skews the Treg-Th17 balance during fungal infection.

## Discussion

The factors that control the tolerogenic phenotype of DCs and its impact on T cell differentiation are unclear. In this study, we elucidated the effect of Zn on regulating DC phenotype. Zn triggered tolerogenicity in DCs by inducing PD-L2, CD103 and IDO and skewed the Treg-Th17 balance *in vivo* in favor of Tregs in *H. capsulatum* infected mice. We reveal that the induction of tolerogenic DCs by Zn was associated with a decrease in proinflammatory cytokines upon fungal challenge and stimulation with TLR ligands. Thus, Zn programs the phenotype and function of DCs to exert tolerogenicity.

DC activation with proinflammatory stimuli escalates surface MHCII by depletion of intracellular free Zn, highlighting a role for Zn in regulating DC maturation (9). Our data is in agreement with this finding, and demonstrates that exogenous Zn suppresses surface MHCII on DCs *in vitro* and *in vivo*. Importantly, Zn induces co-inhibitory markers in DCs to promote the development of a tolerogenic phenotype. The suppression of DC activation caused by reduced MHCII points to a role for Zn in “locking” DCs in the immature state, thereby limiting their ability to present antigens to T cells and drive effector T cell responses.

Tolerogenic DCs express PD-L1, PD-L2 and immunosuppressive mediators such as IDO, TGF $\beta$  and IL-10 (10). T cell activation and tolerance are regulated by these co-inhibitory molecules and immunosuppressive factors. Zn induced a shift in the expression of MHCII from MHCII<sup>hi</sup> to MHCII<sup>lo</sup> and preferentially triggered PD-L2 in MHCII<sup>lo</sup> DCs *in vitro*. Likewise, Zn dampened MHCII expression on DCs *in vivo* and elevated PD-L1 and PD-L2 specifically in the MHCII<sup>lo</sup> DC population. PD ligands on DCs engage PD-1 receptor on T cells to promote Treg differentiation and T cell exhaustion (27, 28). In this context, elevated IDO and PD-L2 in DCs exposed to Zn, in combination with diminished MHCII may contribute to inhibitory signals that subsequently elevate Treg differentiation *in vivo*. The engagement of PD-L1 and PD-L2 expressing tolerogenic DCs with T cells may constrict

proinflammatory DC – T cell interactions to limit a sustained effector T cell response. PD-L1 and PD-L2 regulate immune responses to infectious agents. PD-1 blockade increases survival of mice lethally infected with *H. capsulatum* suggesting that a functional PD1-PDL pathway is required for fungal persistence and dissemination (29). Engagement of the PD-L/PD1 pathway results in weak antimicrobial responses, but plays a critical role in immunosuppression (30). Our findings reveal that regulation of the DC phenotype by Zn may modulate the PD-L2 – PD-1 axis that has important implications in inflammation control.

IDO produced by DCs suppresses effector T cells and induces Tregs by a dual mechanism. The enzyme renders tryptophan unavailable for T cell proliferation and survival and generates toxic kynurenine to drive effector T cell apoptosis (31). Kynurenine metabolites exert cytotoxicity on effector T, B and NK cells without affecting DCs (31). We uncovered a role for Zn in tryptophan starvation by IDO-producing DCs suggesting that this metal could alter the metabolic milieu during T cell differentiation. Although, tolerogenic markers were increased in response to Zn in the MHCII<sup>lo</sup> population, Zn comparably induced IDO in MHCII<sup>hi</sup> and MHCII<sup>lo</sup> DCs. Exposure of MHCII<sup>hi</sup> DCs to Zn possibly decreased MHCII expression, leading to an IDO response similar to that of MHCII<sup>lo</sup> DCs. Nonetheless, total DCs and MHCII<sup>lo</sup> DCs comparably degraded tryptophan and produced kynurenines in response to Zn. Moreover, IDO induction was specific to Zn, as another divalent cation, iron, failed to trigger IDO in DCs.

A number of signaling pathways govern IDO regulation (27, 28). IRF8 and IFNAR were necessary for *Ido1* expression in response to Zn and *H. capsulatum* infection. IRF8 transcriptionally induces *Ido1* and its regulation by Zn can be explained by two possibilities (20). First, Zn may directly induce IDO upregulation via IRF8. Second, IRF8 activates the IFN  $\alpha/\beta$  promoter that in turn mediates autocrine signaling via IFNAR to drive IDO (32). However, *Ifnb* was elevated only upon infection with *H. capsulatum* and not upon Zn treatment. Nonetheless, our data indicate that IRF8 and IFNAR signaling regulate Zn driven expression of IDO, but the molecular cues involved need to be determined.

Tolerogenic DCs manifest subdued antigen presentation and proinflammatory responses to TLR ligands. (10). This prompted us to investigate the response of Zn-treated DCs upon TLR challenge. DCs recognize microbial pathogen associated molecular patterns (PAMPs) via TLRs to recruit adaptor proteins resulting in nuclear factor NF- $\kappa$ B activation to initiate proinflammatory responses. Zn differentially modulates MyD88 and TRIF, where an early Zn signal facilitates MyD88, but limits TRIF signaling (33). The MyD88 pathway is common to all TLRs except TLR3 that engages TRIF (23, 34, 35). Our data demonstrate that Zn curtails proinflammatory responses induced by TLRs that signal via both MyD88 dependent and independent pathways and also upon fungal infection. This finding demonstrates that Zn induces DC tolerogenicity broadly in response to bacterial, fungal and viral antigens to suppress inflammation. Zn inhibits I $\kappa$ B kinase (IKK) and NF- $\kappa$ B downstream of MyD88 that could potentially attenuate a TLR4 response by dephosphorylation of these phosphate dependent kinases. This mechanism may explain downregulation of NF- $\kappa$ B targets in DCs in the presence of Zn (36). Zn did not alter the TLR4 surface expression on DCs providing evidence that the metal inhibits targets

downstream of the receptor. These findings may be extended to understanding the significance of Zn in controlling inflammation in conditions such as sepsis (37).

Unrestrained infection leads to hyperinflammation. For example, transient plasma Zn deficiency in sepsis aggravates inflammatory cytokine production and mortality, while Zn supplementation partially restores protection (38, 39). The cytokines produced by DCs initiate autocrine feedback mechanisms that maintain DC activation (40). Our finding that Zn modulates the proinflammatory response and phenotype of DCs upon fungal infection or TLR challenge, suggests that manipulation of the cytokine environment by this metal may impact autocrine feedback mechanisms leading to control of the DC activation state. Thus, Zn supplementation may serve as a potential therapeutic to dampen proinflammatory responses by DCs.

In agreement with *in vitro* findings, Zn increased *Ido1* expression in lung leukocytes, but the contributing populations are currently unknown. Nonetheless, MHCII suppression on DCs, elevated *Ido1* and *Raldh1* expression in the lungs of Zn treated mice indicate the development of a tolerogenic phenotype specific to the site of infection. IDO induction by Zn may shape an environment favouring Treg differentiation *in vivo*. Retinoic acid acts on DCs to induce arginase 1. These DCs exhibit tolerogenicity and promote Foxp3<sup>+</sup> Treg differentiation (41, 42). Our data reveal that Zn has a similar effect on *Arg1*, supporting a role for Zn in shaping the suppressor phenotype of DCs. Thus, in addition to *Ido1* and *Raldh1*, the expression of *Arg1* triggered by Zn may contribute to the skewed Treg-Th17 balance observed *in vivo*.

Zn inhibits STAT3 activation that attenuates Th17 differentiation and promotes Tregs by inhibiting the Sirt-1 deacetylase, an enzyme that maintains FoxP3 stability (43–45). Zn supplementation skewed the Treg-Th17 balance *in vivo* without affecting Th1 or Th2 responses. The shift in Th17-Treg proportions may have resulted from direct action of Zn on T cells or an indirect effect through the emergence of tolerogenic DCs. Our data support the latter, as Zn did not directly induce FoxP3 expression in naïve T cells or in the presence of Treg inducing cytokines. However, the direct impact of Zn on T cells cannot be ruled out *in vivo* and warrants further investigation. Importantly, the effects of Zn on Tregs became evident during later stages of Zn supplementation and acute infection. These changes were not observed during the resolution phase suggesting that the effects of exogenous Zn administration were most profound during the course of disease progression.

Th17 cells promote immunity against fungal pathogens (46, 47). Despite an altered Treg-Th17 balance, Zn supplementation did not impair resistance to *H. capsulatum*. This fungal pathogen elicits a Th1 dominant response that facilitates clearance of infection (48). However, when Th1 immunity is compromised, Th17 responses play a crucial role in elimination of the pathogen (49, 50). *H. capsulatum* infected mice exposed to Zn specifically modulated the proportions of Th17 cells and Tregs, but maintained an intact Th1 response. The data indicate that Zn specifically shapes the Th17:Treg balance without altering Th1 immunity to *H. capsulatum* and provides a possible explanation to comparable fungal clearance in Zn supplemented mice. It is also possible that Zn supplementation prompted

sequestration of the metal by Zn binding proteins such as metallothioneins that contribute to antifungal immunity. (51, 52).

In summary, our data reveal that Zn programmed a tolerogenic phenotype in DCs. Zn decreased MHCII surface expression to enhance the proportion of MHCII<sup>lo</sup> DCs and promoted tolerogenic markers in this population. Modulation of the DC phenotype by Zn resulted in failure to mount a proinflammatory response to fungal infection and bacterial as well as viral antigens. Our data establish the physiological relevance of Zn supplementation on inducing a tolerogenic DC phenotype and skewing the Treg-Th17 balance *in vivo* upon infection with an intracellular fungal pathogen. Of note, the suppressive potential of CD8 $\alpha$ <sup>+</sup> DCs and plasmacytoid DCs has been described (10). Whether Zn influences the tolerogenic mechanisms of these DC subpopulations and its impact on Treg mediated suppression needs to be explored. Nonetheless, our findings suggest that the emergence of tolerogenic DCs and Tregs by Zn supplementation can be favourably employed in immunosuppression and treatment of autoimmune diseases. Thus, manipulating physiological Zn homeostasis could serve as an attractive therapeutic strategy to alter specific functions of immune cells and promote tolerance or suppressive immunity.

## Supplementary Material

Refer to Web version on PubMed Central for supplementary material.

## Acknowledgments

K.S.V is supported by American Heart Association grant 15POST25700182, 2015 and CEG NIEHS P30ES006096. This work was supported by NIH grant AI106269.

We thank Dr. Dr. Harinder Singh and Dr. Edith Jannsen at Cincinnati Children's Hospital and Medical Center for providing *Irf8*<sup>-/-</sup> and *Ifnar1*<sup>-/-</sup> mice, and Agilent Technologies for HPLC.

## Abbreviations

|              |   |
|--------------|---|
| <b>DCs</b>   | Dendritic cells                           |
| <b>MHCII</b> | Major histocompatibility complex class II |
| <b>LPS</b>   | Lipopolysaccharide                        |
| <b>Tregs</b> | Regulatory T cells                        |
| <b>PD-L1</b> | Programmed death-ligand 1                 |
| <b>PD-L2</b> | Programmed death-ligand 2                 |
| <b>IDO</b>   | Indoleamine 2,3-dioxygenase               |
| <b>FoxP3</b> | Forkhead box P3                           |
| <b>Hc</b>    | <i>Histoplasma capsulatum</i>             |
| <b>IRF8</b>  | Interferon regulatory factor 8            |

|                      |                                  |
|----------------------|----------------------------------|
| <b><i>Ifnar1</i></b> | Interferon-alpha/beta receptor 1 |
| <b>NOS2</b>          | Nitric oxide synthase 2          |
| <b>RALDH</b>         | Retinaldehyde dehydrogenase      |

## References

- Shortman K, Naik SH. Steady-state and inflammatory dendritic-cell development. *Nat Rev Immunol.* 2007; 7:19–30. [PubMed: 17170756]
- Steinman RM, Hawiger D, Nussenzweig MC. Tolerogenic dendritic cells. *Annu Rev Immunol.* 2003; 21:685–711. [PubMed: 12615891]
- Prasad AS. Zinc and immunity. *Mol Cell Biochem.* 1998; 188:63–69. [PubMed: 9823012]
- Hirano T, Murakami M, Fukada T, Nishida K, Yamasaki S, Suzuki T. Roles of zinc and zinc signaling in immunity: zinc as an intracellular signaling molecule. *Adv Immunol.* 2008; 97:149–176. [PubMed: 18501770]
- Prasad AS. Effects of zinc deficiency on Th1 and Th2 cytokine shifts. *J Infect Dis.* 2000; 182(Suppl 1):S62–68. [PubMed: 10944485]
- Bao S, Liu MJ, Lee B, Besecker B, Lai JP, Guttridge DC, Knoell DL. Zinc modulates the innate immune response in vivo to polymicrobial sepsis through regulation of NF-kappaB. *Am J Physiol Lung Cell Mol Physiol.* 2010; 298:L744–754. [PubMed: 20207754]
- Stafford SL, Bokil NJ, Achard ME, Kapetanovic R, Schembri MA, McEwan AG, Sweet MJ. Metal ions in macrophage antimicrobial pathways: emerging roles for zinc and copper. *Biosci Rep.* 2013:33.
- Tan JK, O'Neill HC. Maturation requirements for dendritic cells in T cell stimulation leading to tolerance versus immunity. *J Leukoc Biol.* 2005; 78:319–324. [PubMed: 15809288]
- Kitamura H, Morikawa H, Kamon H, Iguchi M, Hojyo S, Fukada T, Yamashita S, Kaisho T, Akira S, Murakami M, Hirano T. Toll-like receptor-mediated regulation of zinc homeostasis influences dendritic cell function. *Nat Immunol.* 2006; 7:971–977. [PubMed: 16892068]
- Maldonado RA, von Andrian UH. How tolerogenic dendritic cells induce regulatory T cells. *Adv Immunol.* 2010; 108:111–165. [PubMed: 21056730]
- Liang L, Sha WC. The right place at the right time: novel B7 family members regulate effector T cell responses. *Curr Opin Immunol.* 2002; 14:384–390. [PubMed: 11973139]
- Mellor A. Indoleamine 2,3 dioxygenase and regulation of T cell immunity. *Biochem Biophys Res Commun.* 2005; 338:20–24. [PubMed: 16157293]
- Kauffman CA, Israel KS, Smith JW, White AC, Schwarz J, Brooks GF. Histoplasmosis in immunosuppressed patients. *Am J Med.* 1978; 64:923–932. [PubMed: 350045]
- Gildea LA, Morris RE, Newman SL. *Histoplasma capsulatum* yeasts are phagocytosed via very late antigen-5, killed, and processed for antigen presentation by human dendritic cells. *J Immunol.* 2001; 166:1049–1056. [PubMed: 11145684]
- Widner B, Werner ER, Schennach H, Wachter H, Fuchs D. Simultaneous Measurement of Serum Tryptophan and Kynurenine by HPLC. *Clinical Chemistry.* 1997; 43:2424–2426. [PubMed: 9439467]
- Kilshaw PJ. Expression of the mucosal T cell integrin alpha M290 beta 7 by a major subpopulation of dendritic cells in mice. *Eur J Immunol.* 1993; 23:3365–3368. [PubMed: 8258351]
- Coombes JL, Siddiqui KR, Arancibia-Carcamo CV, Hall J, Sun CM, Belkaid Y, Powrie F. A functionally specialized population of mucosal CD103+ DCs induces Foxp3+ regulatory T cells via a TGF-beta and retinoic acid-dependent mechanism. *J Exp Med.* 2007; 204:1757–1764. [PubMed: 17620361]
- Asano N, Watanabe T, Kitani A, Fuss IJ, Strober W. Notch1 signaling and regulatory T cell function. *J Immunol.* 2008; 180:2796–2804. [PubMed: 18292500]
- Yan Y, Zhang GX, Gran B, Fallarino F, Yu S, Li H, Cullimore ML, Rostami A, Xu H. IDO upregulates regulatory T cells via tryptophan catabolite and suppresses encephalitogenic T cell

- responses in experimental autoimmune encephalomyelitis. *J Immunol.* 2010; 185:5953–5961. [PubMed: 20944000]
20. Orabona C, Puccetti P, Vacca C, Biccato S, Luchini A, Fallarino F, Bianchi R, Velardi E, Perruccio K, Velardi A, Bronte V, Fioretti MC, Grohmann U. Toward the identification of a tolerogenic signature in IDO-competent dendritic cells. *Blood.* 2006; 107:2846–2854. [PubMed: 16339401]
  21. Jansen M, Reinhard JF Jr. Interferon response heterogeneity: activation of a pro-inflammatory response by interferon alpha and beta. A possible basis for diverse responses to interferon beta in MS. *J Leukoc Biol.* 1999; 65:439–443. [PubMed: 10204571]
  22. Hassanain HH, Chon SY, Gupta SL. Differential regulation of human indoleamine 2,3-dioxygenase gene expression by interferons-gamma and -alpha. Analysis of the regulatory region of the gene and identification of an interferon-gamma-inducible DNA-binding factor. *J Biol Chem.* 1993; 268:5077–5084. [PubMed: 8444884]
  23. Adachi O, Kawai T, Takeda K, Matsumoto M, Tsutsui H, Sakagami M, Nakanishi K, Akira S. Targeted disruption of the MyD88 gene results in loss of IL-1- and IL-18-mediated function. *Immunity.* 1998; 9:143–150. [PubMed: 9697844]
  24. Chua JS, Rofe AM, Coyle P. Dietary zinc supplementation ameliorates LPS-induced teratogenicity in mice. *Pediatr Res.* 2006; 59:355–358. [PubMed: 16492971]
  25. Wong CP, Song Y, Elias VD, Magnusson KR, Ho E. Zinc supplementation increases zinc status and thymopoiesis in aged mice. *J Nutr.* 2009; 139:1393–1397. [PubMed: 19474155]
  26. Sun CM, Hall JA, Blank RB, Bouladoux N, Oukka M, Mora JR, Belkaid Y. Small intestine lamina propria dendritic cells promote de novo generation of Foxp3 T reg cells via retinoic acid. *J Exp Med.* 2007; 204:1775–1785. [PubMed: 17620362]
  27. Liu C, Workman CJ, Vignali DA. Targeting Regulatory T Cells in Tumors. *FEBS J.* 2016
  28. Blackburn SD, Shin H, Haining WN, Zou T, Workman CJ, Polley A, Betts MR, Freeman GJ, Vignali DA, Wherry EJ. Coregulation of CD8+ T cell exhaustion by multiple inhibitory receptors during chronic viral infection. *Nat Immunol.* 2009; 10:29–37. [PubMed: 19043418]
  29. Lazar-Molnar E, Gacser A, Freeman GJ, Almo SC, Nathenson SG, Nosanchuk JD. The PD-1/PD-L costimulatory pathway critically affects host resistance to the pathogenic fungus *Histoplasma capsulatum*. *Proc Natl Acad Sci U S A.* 2008; 105:2658–2663. [PubMed: 18268348]
  30. Salama AD, Chitnis T, Imitola J, Ansari MJ, Akiba H, Tushima F, Azuma M, Yagita H, Sayegh MH, Khoury SJ. Critical role of the programmed death-1 (PD-1) pathway in regulation of experimental autoimmune encephalomyelitis. *J Exp Med.* 2003; 198:71–78. [PubMed: 12847138]
  31. Terness P, Bauer TM, Rose L, Dufter C, Watzlik A, Simon H, Opelz G. Inhibition of allogeneic T cell proliferation by indoleamine 2,3-dioxygenase-expressing dendritic cells: mediation of suppression by tryptophan metabolites. *J Exp Med.* 2002; 196:447–457. [PubMed: 12186837]
  32. Tailor P, Tamura T, Kong HJ, Kubota T, Kubota M, Borghi P, Gabriele L, Ozato K. The feedback phase of type I interferon induction in dendritic cells requires interferon regulatory factor 8. *Immunity.* 2007; 27:228–239. [PubMed: 17702615]
  33. Brieger A, Rink L, Haase H. Differential regulation of TLR-dependent MyD88 and TRIF signaling pathways by free zinc ions. *J Immunol.* 2013; 191:1808–1817. [PubMed: 23863901]
  34. Horng T, Barton GM, Flavell RA, Medzhitov R. The adaptor molecule TIRAP provides signalling specificity for Toll-like receptors. *Nature.* 2002; 420:329–333. [PubMed: 12447442]
  35. Yamamoto M, Sato S, Mori K, Hoshino K, Takeuchi O, Takeda K, Akira S. Cutting edge: a novel Toll/IL-1 receptor domain-containing adapter that preferentially activates the IFN-beta promoter in the Toll-like receptor signaling. *J Immunol.* 2002; 169:6668–6672. [PubMed: 12471095]
  36. Uzzo RG, Crispin PL, Golovine K, Makhov P, Horwitz EM, Kolenko VM. Diverse effects of zinc on NF-kappaB and AP-1 transcription factors: implications for prostate cancer progression. *Carcinogenesis.* 2006; 27:1980–1990. [PubMed: 16606632]
  37. Tucci M, Stucci S, Strippoli S, Silvestris F. Cytokine overproduction, T-cell activation, and defective T-regulatory functions promote nephritis in systemic lupus erythematosus. *J Biomed Biotechnol.* 2010; 2010:457146. [PubMed: 20671931]
  38. Knoell DL, Julian MW, Bao S, Besecker B, Macre JE, Leikauf GD, DiSilvestro RA, Crouser ED. Zinc deficiency increases organ damage and mortality in a murine model of polymicrobial sepsis. *Crit Care Med.* 2009; 37:1380–1388. [PubMed: 19242332]

39. Gaetke LM, McClain CJ, Talwalkar RT, Shedlofsky SI. Effects of endotoxin on zinc metabolism in human volunteers. *Am J Physiol.* 1997; 272:E952–956. [PubMed: 9227437]
40. Pollara G, Handley ME, Kwan A, Chain BM, Katz DR. Autocrine type I interferon amplifies dendritic cell responses to lipopolysaccharide via the nuclear factor-kappaB/p38 pathways. *Scand J Immunol.* 2006; 63:151–154. [PubMed: 16499567]
41. Chang J, Thangamani S, Kim MH, Ulrich B, Morris SM Jr, Kim CH. Retinoic acid promotes the development of Arg1-expressing dendritic cells for the regulation of T-cell differentiation. *Eur J Immunol.* 2013; 43:967–978. [PubMed: 23322377]
42. Bhatt S, Qin J, Bennett C, Qian S, Fung JJ, Hamilton TA, Lu L. All-trans retinoic acid induces arginase-1 and inducible nitric oxide synthase-producing dendritic cells with T cell inhibitory function. *J Immunol.* 2014; 192:5098–5108. [PubMed: 24790153]
43. Rosenkranz E, Metz CH, Maywald M, Hilgers RD, Wessels I, Senff T, Haase H, Jager M, Ott M, Aspinnall R, Plumakers B, Rink L. Zinc supplementation induces regulatory T cells by inhibition of Sirt-1 deacetylase in mixed lymphocyte cultures. *Mol Nutr Food Res.* 2015
44. Kitabayashi C, Fukada T, Kanamoto M, Ohashi W, Hojyo S, Atsumi T, Ueda N, Azuma I, Hirota H, Murakami M, Hirano T. Zinc suppresses Th17 development via inhibition of STAT3 activation. *Int Immunol.* 2010; 22:375–386. [PubMed: 20215335]
45. Rosenkranz E, Hilgers RD, Uciechowski P, Petersen A, Plumakers B, Rink L. Zinc enhances the number of regulatory T cells in allergen-stimulated cells from atopic subjects. *Eur J Nutr.* 2015
46. Lock C, Hermans G, Pedotti R, Brendolan A, Schadt E, Garren H, Langer-Gould A, Strober S, Cannella B, Allard J, Klonowski P, Austin A, Lad N, Kaminski N, Galli SJ, Oksenberg JR, Raine CS, Heller R, Steinman L. Gene-microarray analysis of multiple sclerosis lesions yields new targets validated in autoimmune encephalomyelitis. *Nat Med.* 2002; 8:500–508. [PubMed: 11984595]
47. Lubberts E. The role of IL-17 and family members in the pathogenesis of arthritis. *Curr Opin Investig Drugs.* 2003; 4:572–577.
48. Allendoerfer R, Deepe GS Jr. Intrapulmonary response to *Histoplasma capsulatum* in gamma interferon knockout mice. *Infect Immun.* 1997; 65:2564–2569. [PubMed: 9199420]
49. Kroetz DN, Deepe GS. CCR5 Dictates the Equilibrium of Proinflammatory IL-17+ and Regulatory Foxp3+ T Cells in Fungal Infection. *The Journal of Immunology.* 2010; 184:5224–5231. [PubMed: 20335531]
50. Deepe GS Jr, Gibbons RS. TNF-alpha antagonism generates a population of antigen-specific CD4+CD25+ T cells that inhibit protective immunity in murine histoplasmosis. *J Immunol.* 2008; 180:1088–1097. [PubMed: 18178849]
51. Subramanian Vignesh K, Landero Figueroa JA, Porollo A, Caruso JA, Deepe GS Jr. Granulocyte macrophage-colony stimulating factor induced Zn sequestration enhances macrophage superoxide and limits intracellular pathogen survival. *Immunity.* 2013; 39:697–710. [PubMed: 24138881]
52. Subramanian Vignesh K, Landero Figueroa JA, Porollo A, Caruso JA, Deepe GS Jr. Zinc sequestration: arming phagocyte defense against fungal attack. *PLoS Pathog.* 2013; 9:e1003815. [PubMed: 24385902]



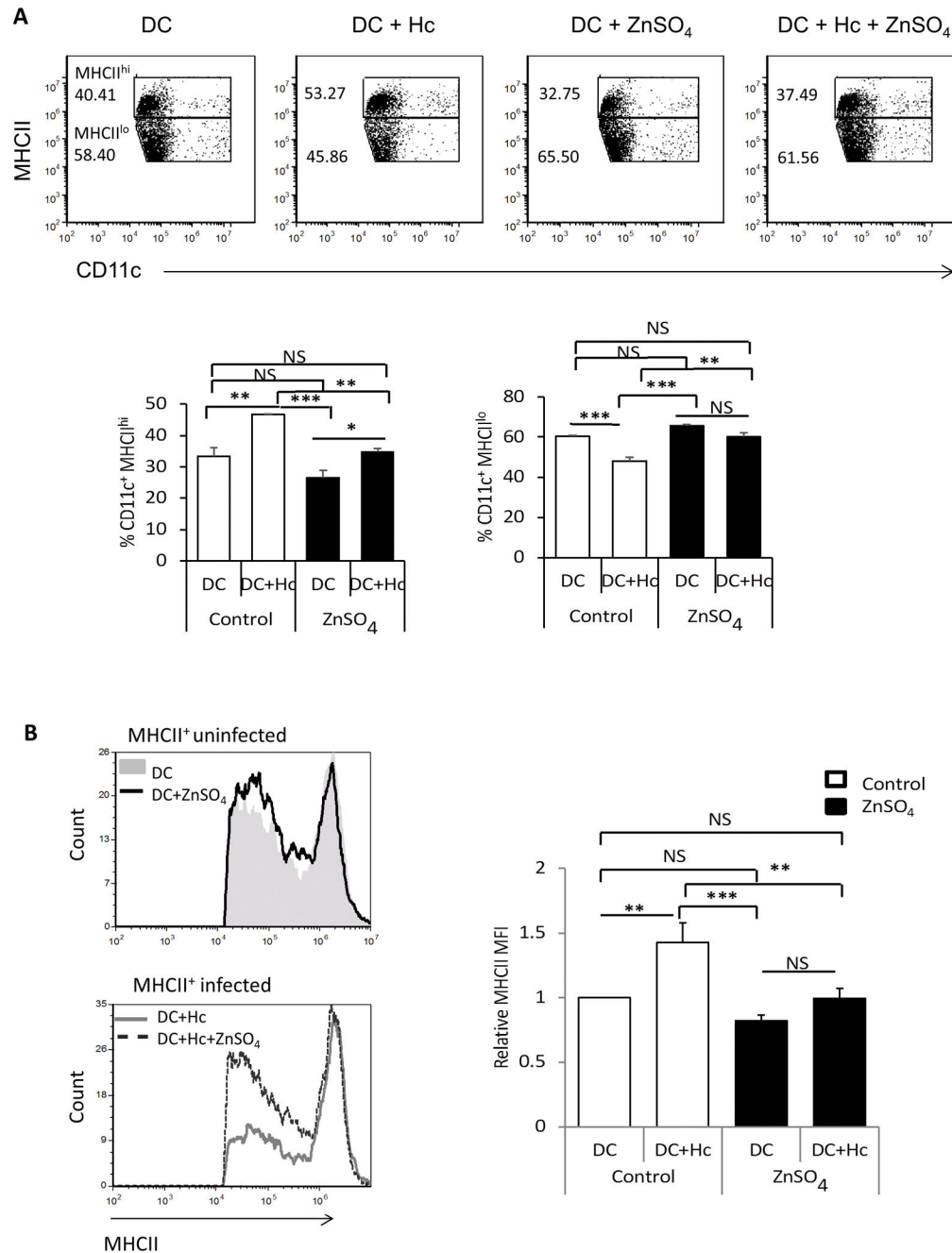


**Fig. 1. Zn decreases the proportion of MHCII<sup>hi</sup> DCs**

**A)** Dot plots of DCs gated as MHCII<sup>hi</sup> and MHCII<sup>lo</sup> populations, numbers in plots are percent values, bar graphs represent quantification of MHCII<sup>hi</sup> and MHCII<sup>lo</sup> CD11c<sup>+</sup> DCs; **B)** MHCII histograms gated on uninfected or *H. capsulatum*-infected CD11c<sup>+</sup> DCs. Graphs are relative MHCII MFI normalized to DC control group, 6 independent experiments; data are mean  $\pm$  SEM, \*  $p < 0.05$ ; \*\*  $p < 0.01$ ; \*\*\*  $p < 0.001$ ; NS, not significant by two way ANOVA.

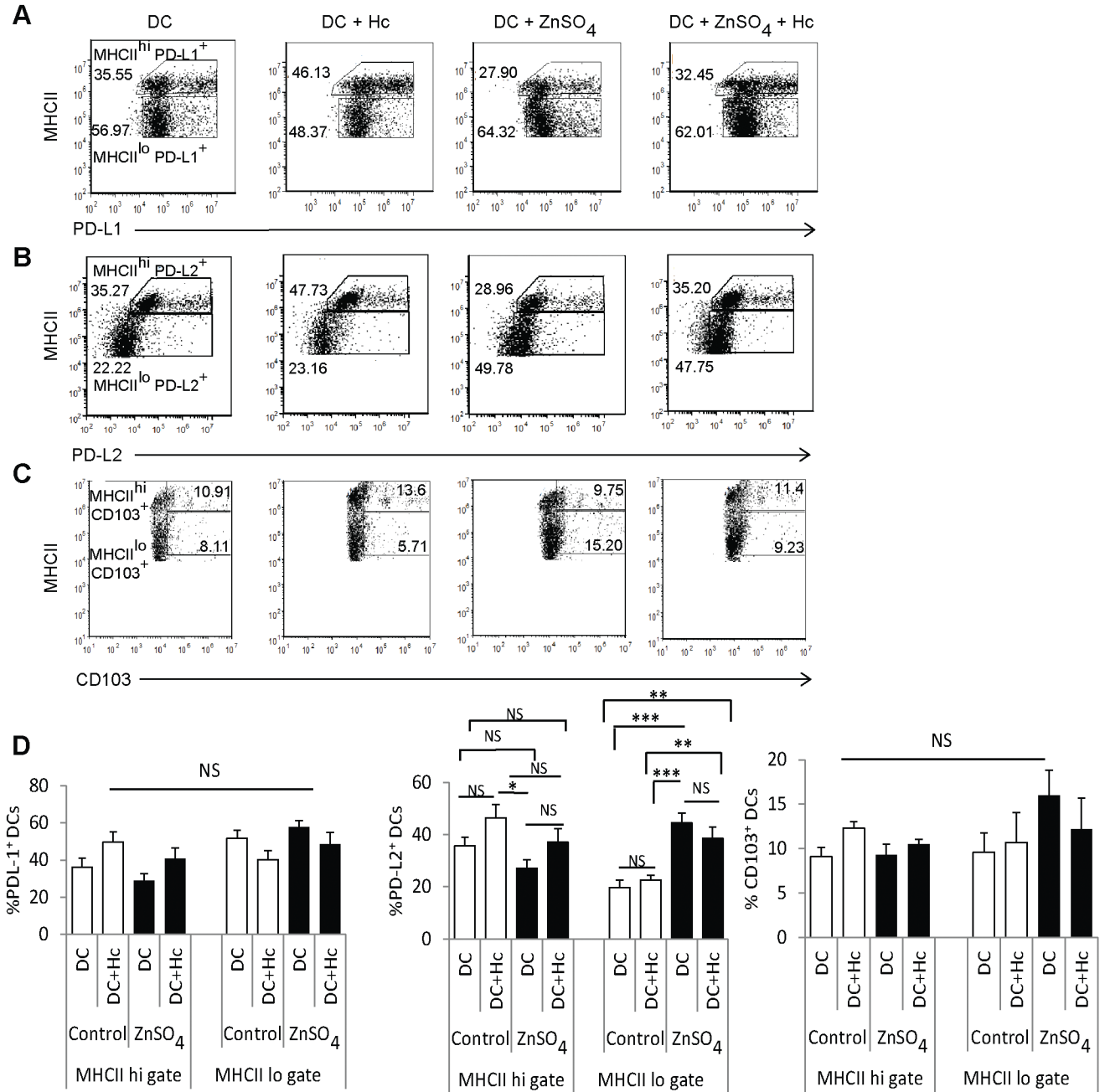


**Fig. 2. Zn shapes tolerogenic DC phenotype**

**A–C)** Dot plots represent PD-L1<sup>+</sup>, PD-L2<sup>+</sup> and CD103<sup>+</sup> DCs in MHCII<sup>hi</sup> and MHCII<sup>lo</sup> gates, numbers in plots are percent values; **D)** Graphical representation of percent PD-L1<sup>+</sup> (4 independent experiments), PDL2<sup>+</sup> (6 independent experiments) and CD103<sup>+</sup> DCs (3 independent experiments) in MHCII<sup>hi</sup> and MHCII<sup>lo</sup> gates; Data presented as mean ± SEM, \* *p* < 0.05; \*\* *p* < 0.01; \*\*\* *p* < 0.001; NS, not significant by two way ANOVA.

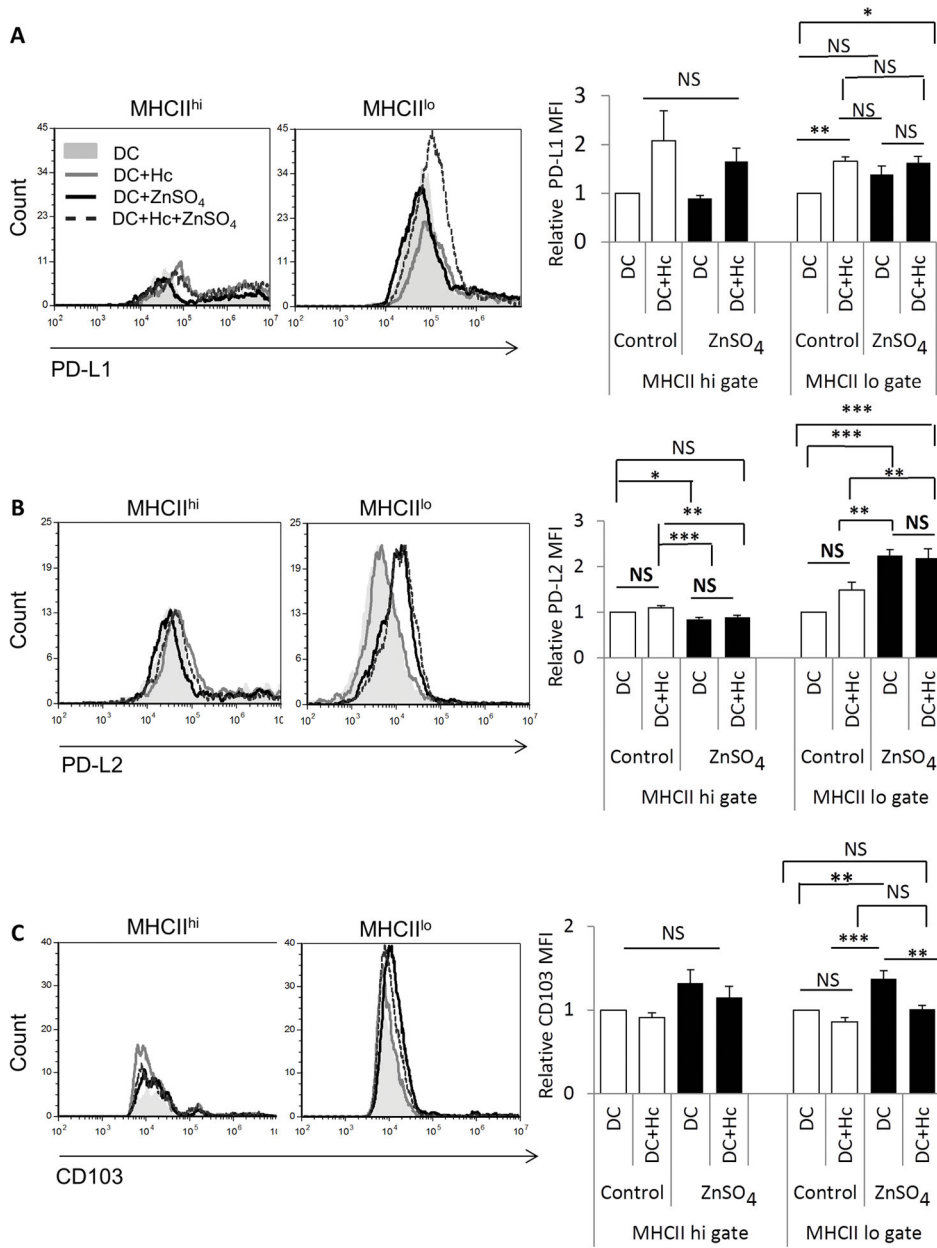


**Fig. 3. Zn escalates the expression of tolerogenic markers**

**A–C)** Histograms representing PD-L1, PD-L2 and CD103 MFI in MHCII<sup>hi</sup> and MHCII<sup>lo</sup> DCs, graphs are relative MFI in MHCII<sup>hi</sup> and MHCII<sup>lo</sup> gates normalized to DC control group, 4–6 independent experiments. Data presented as mean ± SEM, \*  $p < 0.05$ ; \*\*  $p < 0.01$ ; \*\*\*  $p < 0.001$ ; NS, not significant by two way ANOVA.

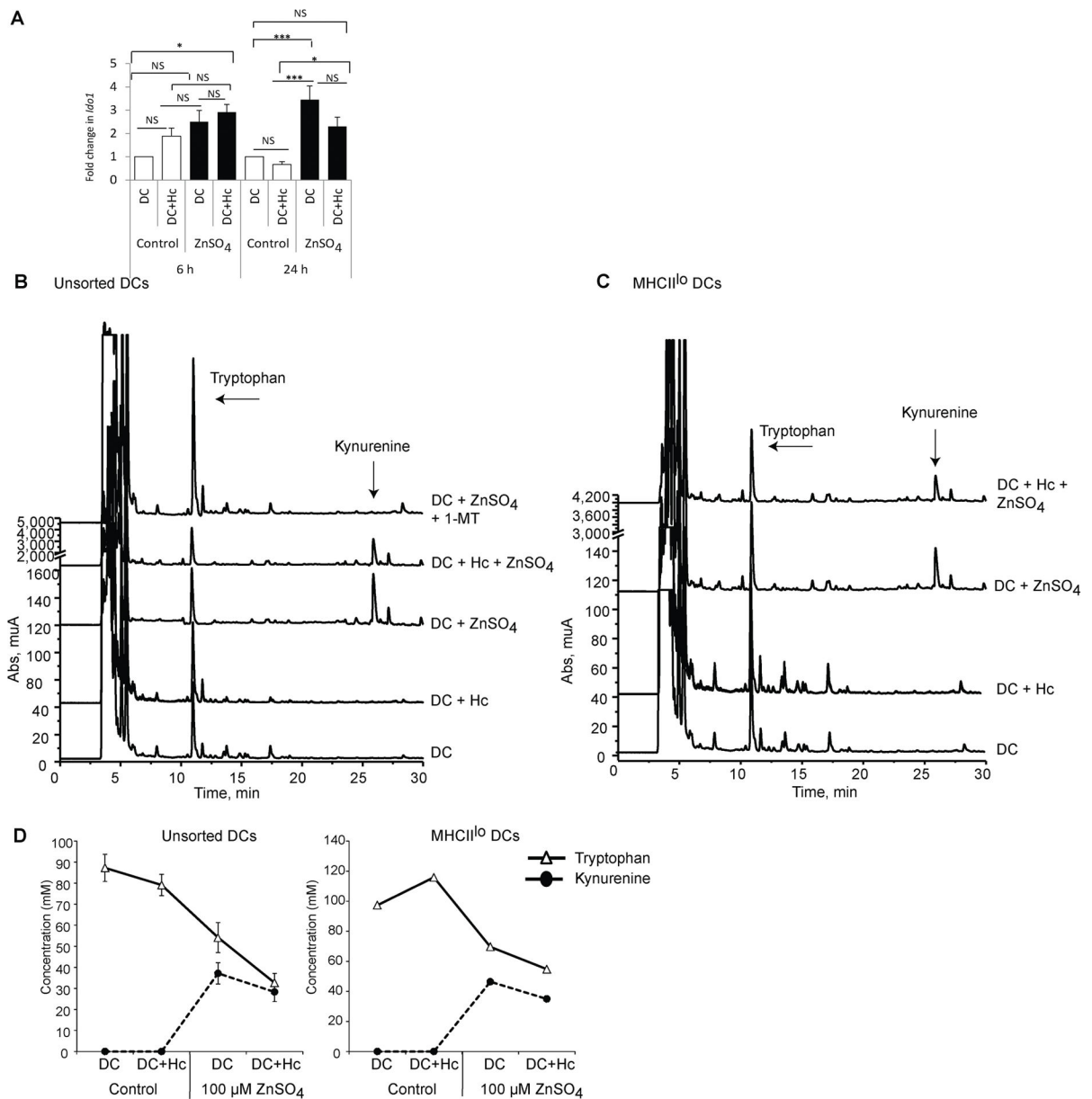


**Fig. 4. Zn triggers IDO activity in DCs**

*Ido1* expression in **A**) control and ZnSO<sub>4</sub> treated DCs in uninfected and infected states for 6 h and 24 h, 12 independent experiments; and **B–C**) Chromatographs representing tryptophan degradation and kynurenine production in unsorted DCs (2 independent experiments) and sorted MHCII<sup>lo</sup> DCs (1 experiment). **D**) Tryptophan degradation and kynurenine production in unsorted DCs, left (2 independent experiments) and MHCII<sup>lo</sup> DCs, right (1 experiment). Solid line with triangles represents tryptophan concentration and dotted line with black circles represents kynurenine concentration in the samples. \*  $p < 0.05$ ; \*\*  $p < 0.01$ ; \*\*\*  $p < 0.001$ ; NS, not significant by two way ANOVA.

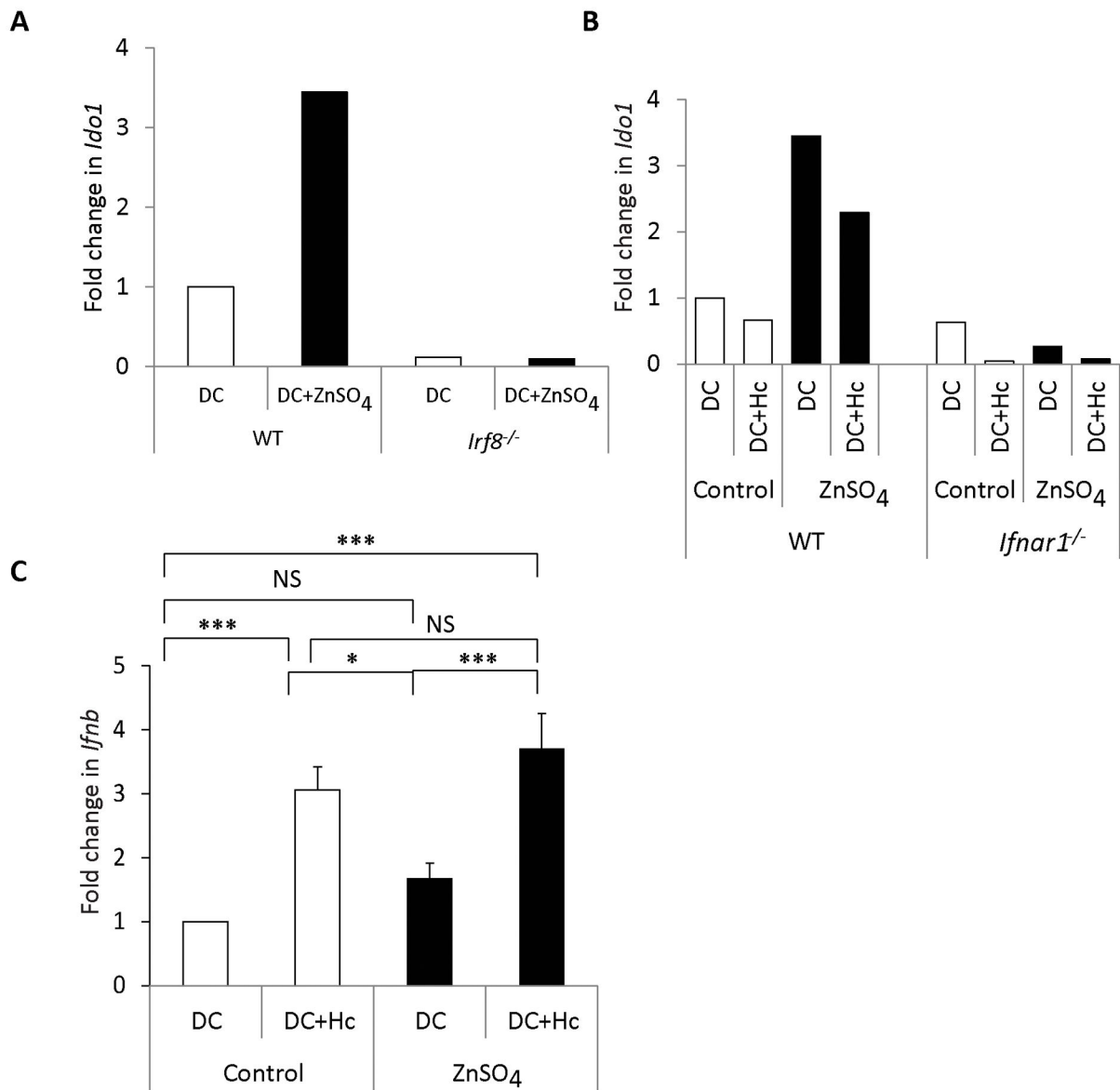


**Fig. 5. IRF8 and IFNAR signaling regulate IDO expression**

**A)** *Ido1* expression 24 h post ZnSO<sub>4</sub> treatment in *Irf8*<sup>-/-</sup> DCs normalized to WT DCs (1 experiment); and **B)** *Ido1* expression in WT and *Ifnar1*<sup>-/-</sup> DCs (1 experiment) 24 h post ZnSO<sub>4</sub> treatment and infection normalized to WT DCs **C)** Fold change in *Ifnb* expression in control and ZnSO<sub>4</sub> treated DCs in uninfected and infected states for 24 h, normalized to DC control group. 3 independent experiments; Data presented as mean ± SEM.

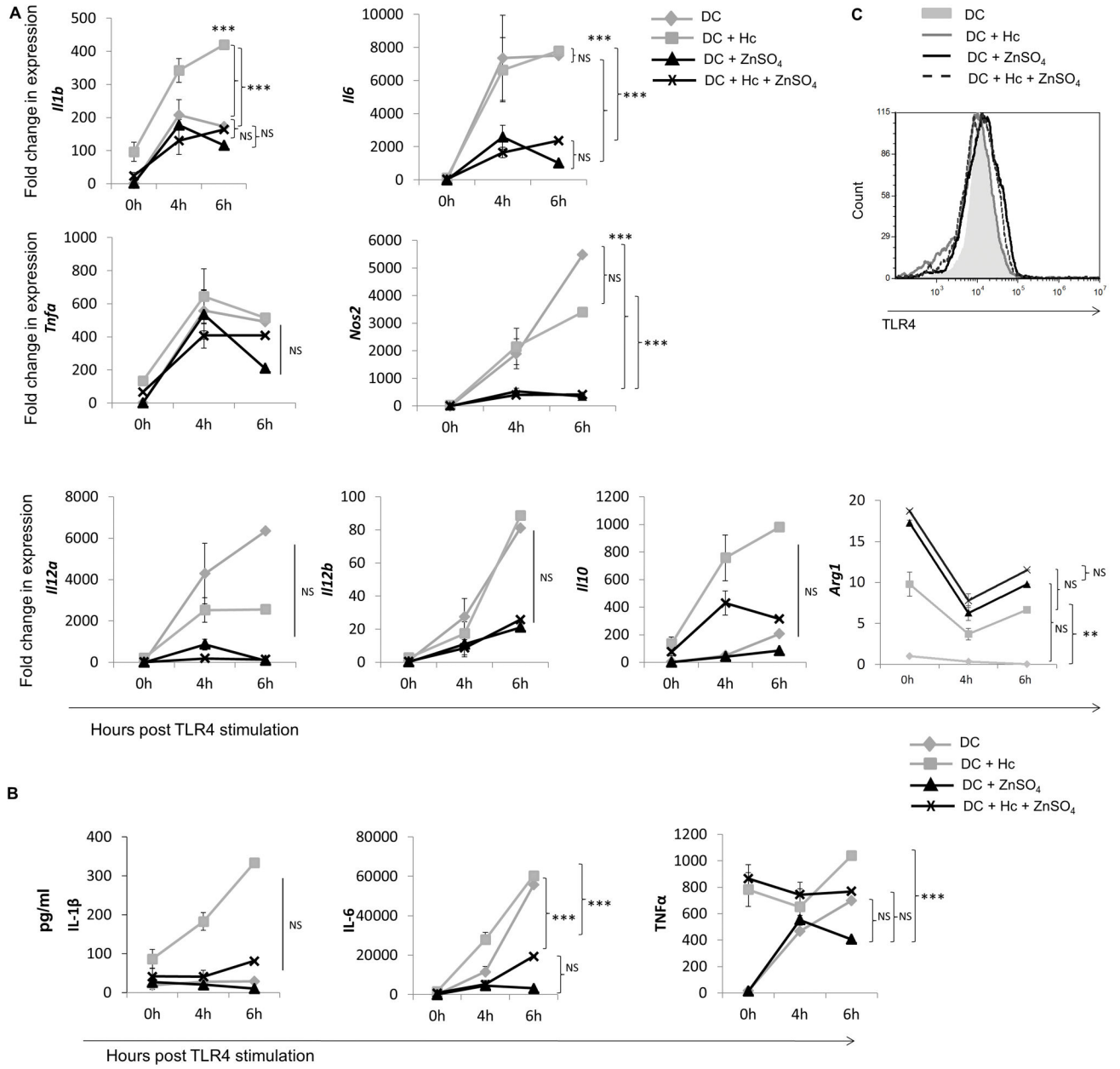


**Fig. 6. Zn suppresses the DC response to LPS and fungal challenge**

DCs were treated with 100  $\mu$ M ZnSO<sub>4</sub> and infected with 0.5 yeasts per DC for 24 h, followed by stimulation with 100 ng/ml LPS for 0, 4 and 6 h.

**A)** Gene expression at 4 and 6 h post TLR4 stimulation normalized to untreated DCs at 0 h, 3 independent experiments; **B)** Cytokine release at 0, 4 and 6 h post TLR4 stimulation in culture supernatants. 3 independent experiments. Statistical analysis presented for 0 h and 4 h time points; and **C)** Histogram of TLR4 expression in DCs. \*  $p < 0.05$ ; \*\*  $p < 0.01$ ; \*\*\*  $p < 0.001$ ; NS, not significant by two way ANOVA.

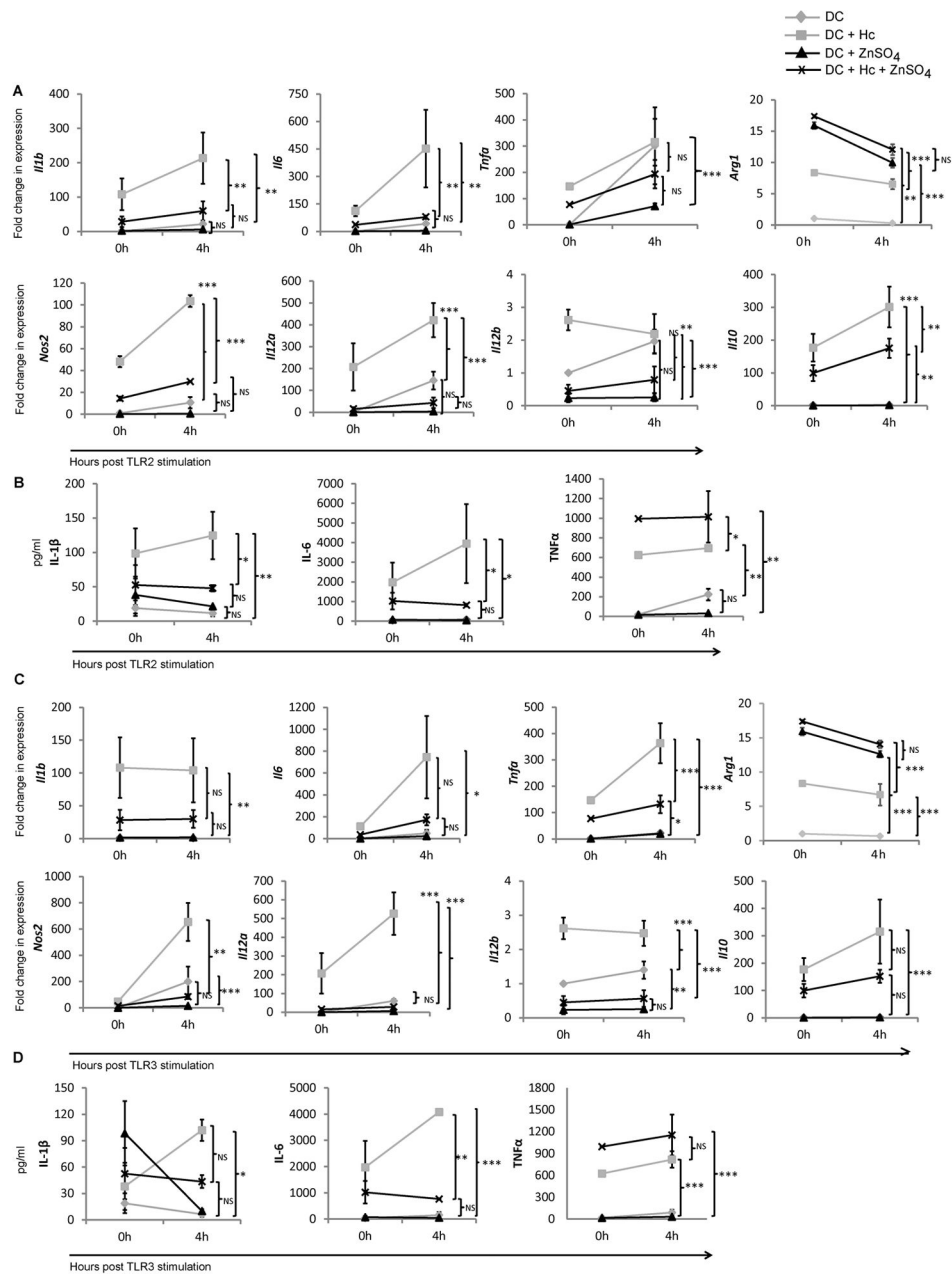


**Fig. 7. Zn inhibits responsiveness to TLR2 and TLR3 stimulation in DCs**

DCs were treated with 100  $\mu$ M ZnSO<sub>4</sub> and infected with 0.5 yeasts per DC for 24 h followed by stimulation with 10  $\mu$ g/ml of the TLR2 ligand, peptidoglycan from *Staphylococcus aureus* (PGN-SA) or 10  $\mu$ g/ml of polyinosinic:polycytidylic acid (Poly I:C) for 0 h and 4 h. **A)** Cytokine expression at 4 h post TLR2 stimulation normalized to untreated DCs at 0 h, 2 independent experiments; **B)** Cytokine release in culture supernatants at 0 h and 4 h post TLR2 stimulation normalized to untreated DCs at 0 h, 2 independent experiments; **C)** Cytokine expression at 4 h post TLR3 stimulation normalized to untreated DCs at 0 h, 2 independent experiments; and **D)** Cytokine release in culture supernatants at 0 h and 4 h post TLR3 stimulation normalized to untreated DCs at 0 h, 2 independent experiments. Data

presented as mean  $\pm$  SEM. \*  $p < 0.05$ ; \*\*  $p < 0.01$ ; \*\*\*  $p < 0.001$ ; NS, not significant by two way ANOVA.

Author Manuscript

Author Manuscript

Author Manuscript

Author Manuscript



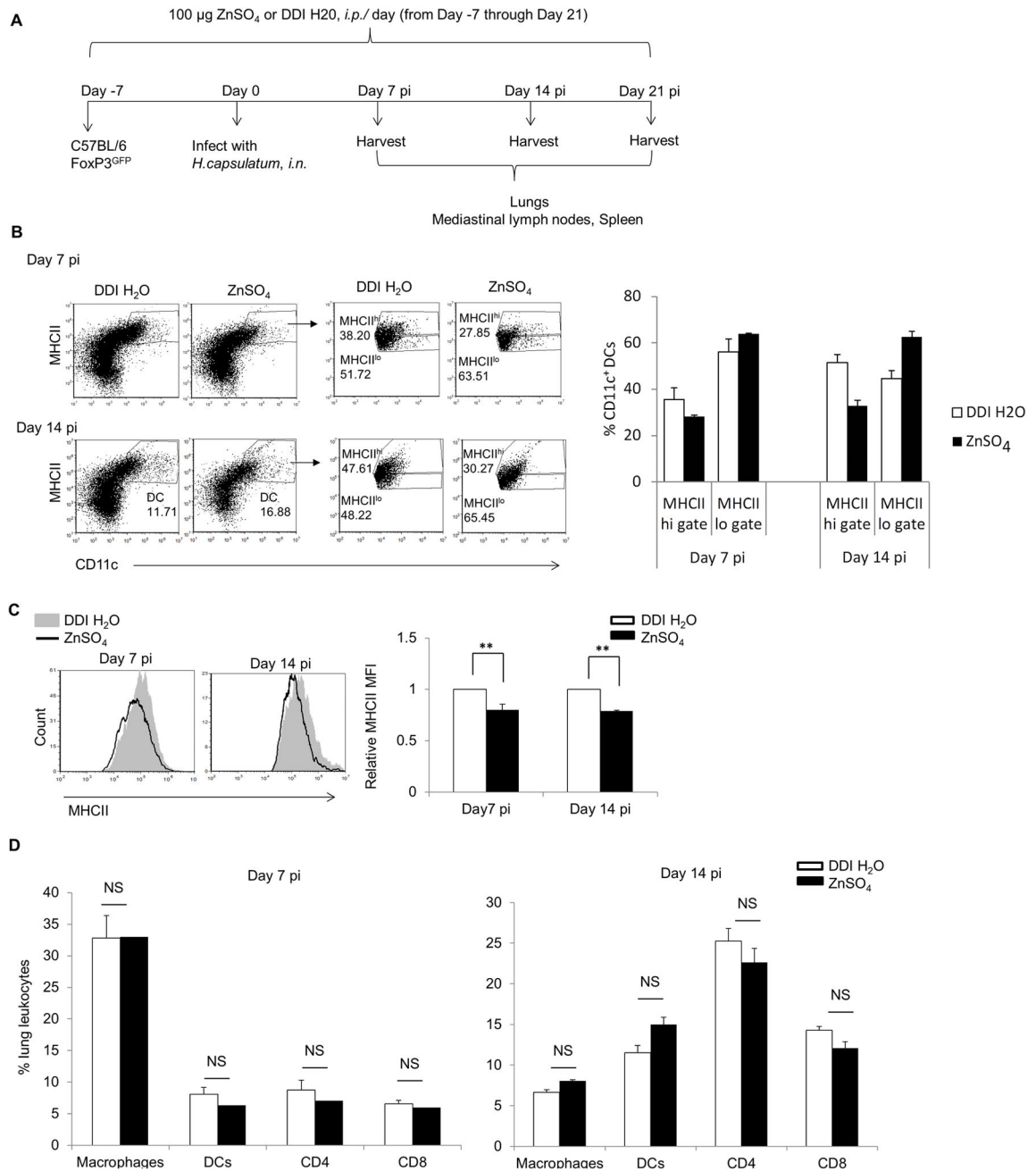


**Fig. 8. Zn suppresses MHCII expression on DCs *in vivo***

**A)** Schematic representation of Zn supplementation and infection, mice treated intraperitoneally (*i.p.*) with DDI  $\text{H}_2\text{O}$  control or 100  $\mu\text{g}$   $\text{ZnSO}_4$ /day for 7 days followed by intranasal infection (*i.n.*) with  $2 \times 10^6$  Hc for 7, 14 or 21 days. Zn or DDI  $\text{H}_2\text{O}$  treatment was continued throughout the period of infection; **B)** Dot plots of CD11c<sup>+</sup> MHCII<sup>+</sup> DCs gated on lung leukocytes obtained at days 7 and 14 post infection (*pi*) (left), MHCII<sup>hi</sup> and MHCII<sup>lo</sup> populations gated on DCs (right), numbers in plots are percent values, bar graphs represent percent CD11c<sup>+</sup> DCs in MHCII<sup>hi</sup> and MHCII<sup>lo</sup> gates in DDI  $\text{H}_2\text{O}$  and  $\text{ZnSO}_4$

treated mice; **C**) Histograms of MHCII expression gated on DCs, relative MHCII MFI of Zn treated mice normalized to DDI H<sub>2</sub>O control mice; and **D**) Percent populations in lung leukocytes in DDI H<sub>2</sub>O and ZnSO<sub>4</sub> treated mice at days 7 and 14 *p.i.*. Data expressed as mean ± SEM, n = 6–8/group, 2 independent experiments, \*  $p < 0.05$ ; \*\*  $p < 0.01$ ; \*\*\*  $p < 0.001$ ; NS, not significant by student's t test.

Author Manuscript

Author Manuscript

Author Manuscript

Author Manuscript

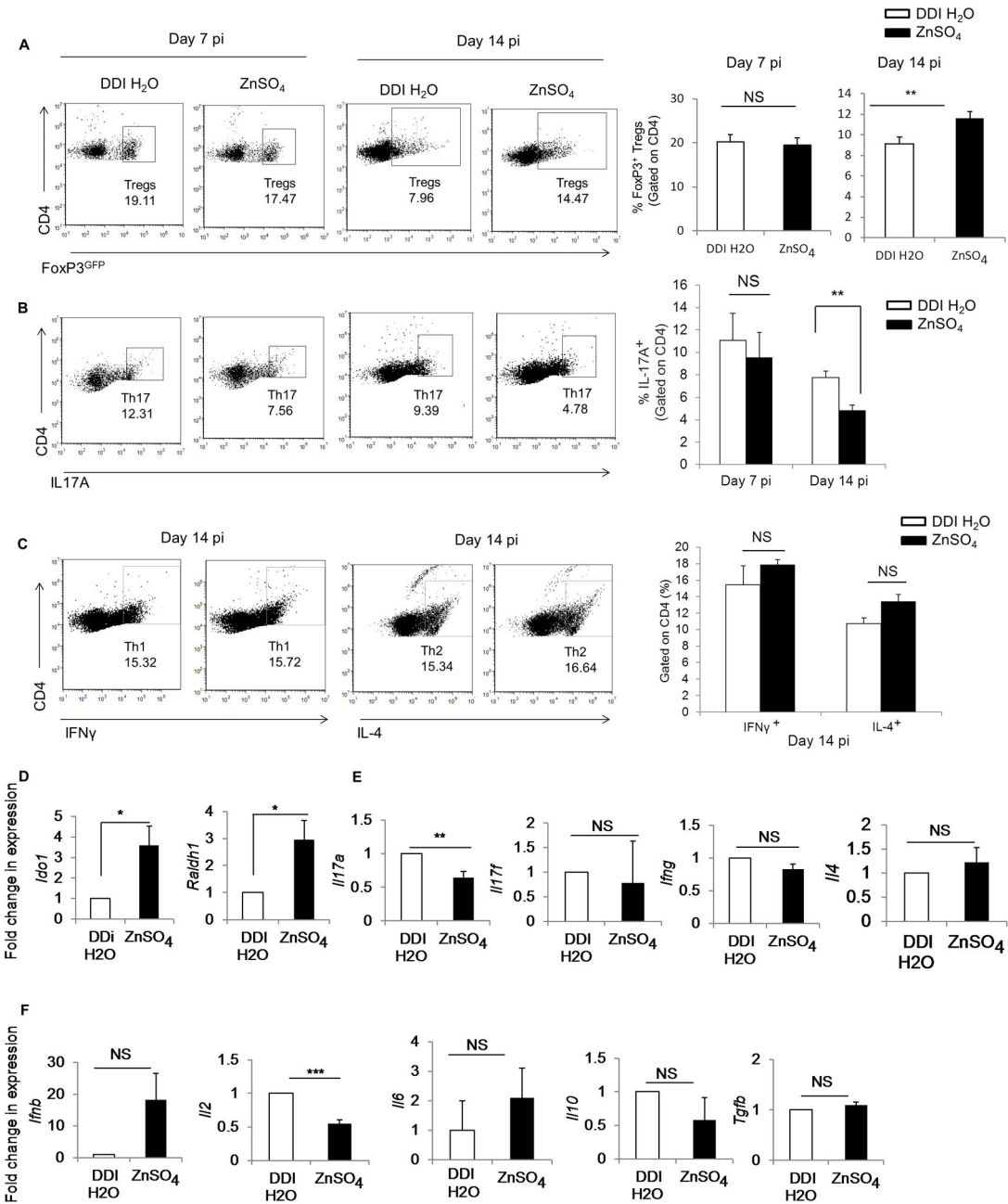


**Fig. 9. Zn skews Treg-Th17 balance during fungal infection *in vivo***

**A)** Dot plots and bar graph of percent FoxP3<sup>+</sup> Tregs gated on CD4<sup>+</sup> lung leukocytes in DDI H<sub>2</sub>O and ZnSO<sub>4</sub> treated mice on days 7 and 14 *p.i.*, 2 independent experiments.; **B)** Dot plots and bar graph of percent Th17 cells gated on CD4<sup>+</sup> lung leukocytes in DDI H<sub>2</sub>O and ZnSO<sub>4</sub> treated mice on days 7 and 14 *p.i.*, n = 4 mice/group for day 7 *p.i.*, n = 8 mice/group for day 14 *p.i.*, 2 independent experiments; **C)** Dot plots of IFN $\gamma$  producing Th1 cells and IL-4 producing Th2 cells gated on CD4<sup>+</sup> lung leukocytes in DDI H<sub>2</sub>O and ZnSO<sub>4</sub> treated mice on day 14 *p.i.*, bar graphs are quantification of IFN $\gamma$ <sup>+</sup> Th1 and IL-4<sup>+</sup> Th2 cells gated on CD4<sup>+</sup> lung leukocytes, n = 4 mice/group; and **D-F)** Gene expression of *Ido1* and *Raldh1*

in whole lung leukocytes of Zn treated mice normalized to DDI H<sub>2</sub>O treated mice on day 14 *p.i.*, (4 mice/group), 2 independent experiments, Data expressed as mean  $\pm$  SEM \*  $p < 0.05$ ; \*\*  $p < 0.01$ ; \*\*\*  $p < 0.001$ ; NS, not significant by student's t test.

Author Manuscript

Author Manuscript

Author Manuscript

Author Manuscript